

1 **The gene expression signature of electrical stimulation in the human brain**

2  
3 Snehajyoti Chatterjee<sup>1,2</sup>, Yann Vanrobaeys<sup>1#</sup>, Annie I Gleason<sup>3#</sup>, Brian J. Park<sup>4</sup>, Shane  
4 A. Heiney<sup>1,2,5</sup>, Ariane E. Rhone<sup>4</sup>, Kirill V. Nourski<sup>4</sup>, Lucy Langmack<sup>1,2</sup>, Budhaditya  
5 Basu<sup>1,2</sup>, Utsav Mukherjee<sup>1,2</sup>, Christopher K. Kovach<sup>4,6</sup>, Zsuzsanna Kocsis<sup>4,7</sup>, Yukiko  
6 Kikuchi<sup>7</sup>, Yaneri A. Ayala<sup>4</sup>, Christopher I. Petkov<sup>4,7</sup>, Marco M. Hefti<sup>8</sup>, Ethan Bahl<sup>3</sup>, Jacob  
7 J Michaelson<sup>3</sup>, Hiroto Kawasaki<sup>4</sup>, Hiroyuki Oya<sup>4</sup>, Matthew A. Howard III<sup>4</sup>, Thomas Nickl-  
8 Jockschat<sup>1,2,3,9,10,11</sup>, Li-Chun Lin<sup>1,2,12</sup>, Ted Abel<sup>1,2,3\*</sup>

9 **Affiliations:**

10 <sup>1</sup>Department of Neuroscience and Pharmacology, Iowa Neuroscience Institute, Carver  
11 College of Medicine, University of Iowa, Iowa City, IA, USA

12 <sup>2</sup>Iowa Neuroscience Institute, University of Iowa, Iowa City, IA, USA

13 <sup>3</sup>Department of Psychiatry, University of Iowa Hospitals and Clinics, Iowa City, IA, USA

14 <sup>4</sup>Department of Neurosurgery, University of Iowa Hospitals and Clinics, Iowa City, IA,  
15 USA

16 <sup>5</sup>Neural Circuits and Behavior Core, Iowa Neuroscience Institute Carver College of  
17 Medicine, University of Iowa, Iowa City, IA, USA

18 <sup>6</sup>Department of Neurosurgery, University of Nebraska Medical Center, Omaha, NE, USA

19 <sup>7</sup>Biosciences Institute, Newcastle University Medical School, Newcastle upon Tyne, UK

20 <sup>8</sup>Department of Pathology, University of Iowa Hospitals and Clinics, Iowa City, IA, USA

21 <sup>9</sup>Department of Psychiatry and Psychotherapy, Otto-von-Guericke University,  
22 Magdeburg, Germany

23 <sup>10</sup>German Center for Mental Health (DZPG), partner site Halle-Jena-Magdeburg,  
24 Germany

25 <sup>11</sup>Center for Intervention and Research on adaptive and maladaptive brain Circuits  
26 underlying mental health (C-I-R-C), Halle-Jena-Magdeburg, Germany

27 <sup>12</sup>Iowa NeuroBank Core, Iowa Neuroscience Institute, Carver College of Medicine,  
28 University of Iowa, Iowa City, IA, USA

29

30 #Authors contributed equally

31 \*Corresponding author:

32 ted-abel@uiowa.edu

33

## Molecular impact of electrical stimulation

34 **Keywords:** Microglia, anterior temporal neocortex, direct electrical stimulation, single  
35 nuclei multiomics

### 36 **Abstract**

37 Direct electrical stimulation has been used for decades as a gold standard clinical tool  
38 to map cognitive function in neurosurgery patients<sup>1-8</sup>. However, the molecular impact of  
39 electrical stimulation in the human brain is unknown. Here, using state-of-the-art  
40 transcriptomic and epigenomic sequencing techniques, we define the molecular  
41 changes in bulk tissue and at the single-cell level in the human cerebral cortex following  
42 direct electrical stimulation of the anterior temporal lobe in patients undergoing  
43 neurosurgery. Direct electrical stimulation surprisingly had a robust and consistent  
44 impact on the expression of genes related to microglia-specific cytokine activity, an  
45 effect that was replicated in mice. Using a newly developed deep learning  
46 computational tool, we further demonstrate cell type-specific molecular activation, which  
47 underscores the effects of electrical stimulation on gene expression in microglia. Taken  
48 together, this work challenges the notion that the immediate impact of electrical  
49 stimulation commonly used in the clinic has a primary effect on neuronal gene  
50 expression and reveals that microglia robustly respond to electrical stimulation, thus  
51 enabling these non-neuronal cells to sculpt and shape the activity of neuronal circuits in  
52 the human brain.

53

54

55

56

57

58

59

60

61

## Molecular impact of electrical stimulation

62

63

### 64 **Main**

65 Electrical stimulation of the human brain has become an indispensable clinical tool for  
66 diagnosis and therapy<sup>1-8</sup>. In neurosurgical patients, cortical stimulation is the gold  
67 standard diagnostic tool to identify the location of functionally relevant brain regions that  
68 are critical for speech, language, or motor function<sup>9,10</sup> to avoid potential damage to  
69 these regions during surgery. Transient changes in gene expression underlie the ability  
70 of the brain to adapt to changes in the environment or brain perturbation, such as  
71 electrical stimulation. Dynamic transcriptomic patterns are essential for cognition<sup>11-13</sup>,  
72 affective processing<sup>14</sup>, addiction<sup>15</sup>, and the initiation of behaviors<sup>16,17</sup>. Thus, electrical  
73 stimulation likely exerts neural effects via alterations in gene expression. Although  
74 diagnostic and therapeutic brain stimulation is conducted daily in thousands of patients  
75 worldwide, the molecular impact of electrical stimulation in the human brain remains  
76 unknown. Recent advances in molecular sequencing techniques have revolutionized  
77 transcriptomics by enabling mapping of changes in transcription and chromatin  
78 accessibility in single cells<sup>18</sup>. However, these experiments have only been conducted in  
79 rodents<sup>19,20</sup> and neurons derived from human induced pluripotent stem cells<sup>21</sup>. A recent  
80 pioneering study utilized a single nuclei molecular approach to link human brain  
81 transcriptomics signatures with oscillatory signatures of memory consolidation in  
82 epileptic patients undergoing an episodic memory task, but these gene expression  
83 measures were obtained many days after assessment of intracranial recording data  
84 during the task<sup>22,23</sup>. Therefore, research is needed to evaluate the more immediate  
85 effects on single-cell early gene expression, such as tens of minutes after neural system  
86 perturbation with electrical stimulation. Studies investigating gene expression profiles  
87 after electrical stimulation are particularly difficult to perform in human brains due to the  
88 requirement that tissue is sampled at precise temporal windows before and after  
89 stimulation.

90 Here, in patients undergoing clinical neurosurgical resection of pathological  
91 epileptogenic sites in the mesial temporal lobe, samples from tissue in the anterior

## Molecular impact of electrical stimulation

92 temporal lobe (ATL) that required clinical resection to access the deeper epileptogenic  
93 site for treatment were obtained before and after electrical stimulation. By analyzing  
94 gene expression at baseline and minutes after stimulation from the same patient, along  
95 with our analysis of samples taken from patients that did not receive electrical  
96 stimulation, we are able to distinguish genes responsive to electrical stimulation from  
97 the genes altered nonspecifically by surgical or disease-based factors that would be  
98 stable across samples. Our parameters for electrical stimulation were based on those  
99 regularly used in clinical mapping<sup>24,25</sup>; moreover, we referenced the human results to a  
100 similar electrical stimulation paradigm in mice, revealing a similar transcriptional profile.  
101 Finally, using a single-nuclei multi-omics approach, we provide insight into the cell-type-  
102 specific transcriptomic and epigenomic responses to electrical stimulation in the human  
103 brain, highlighting important effects beyond neurons, including microglia. This study  
104 provides fundamental insights into changes in cell-type specific molecular signatures in  
105 the human cortex after electrical stimulation, laying the groundwork for a molecular  
106 understanding of the impact of this fundamental tool in clinical neurosurgery, diagnosis,  
107 and treatment.

### 108 **Results**

109 We recruited eight adult neurosurgical patients undergoing surgical resection of seizure  
110 foci following clinical monitoring to treat epilepsy. The patients provided informed  
111 consent to take part in this research and were informed that tissue samples would only  
112 be taken from tissue that would require clinically resection for treatment. The patient  
113 participants underwent an anterior temporal lobectomy for access to a medial temporal  
114 lobe epileptogenic site, during which samples were resected from the neocortex and  
115 processed immediately after removal. The participants were evenly distributed between  
116 two experimental paradigms. In the first group with the electrically stimulated paradigm  
117 (4 participants), a baseline tissue sample was resected from the ATL after the  
118 craniotomy and durotomy, exposing the temporal lobe. Then, an adjacent region of the  
119 cortex was stimulated using a stimulation protocol commonly used for bipolar electrical  
120 stimulation (50 Hz) for 2 minutes<sup>24,25</sup> And resected approximately thirty minutes later  
121 ( $32.5 \pm 11.2$  min), a sample was taken from the stimulated region (**Fig. 1a**;  
122 **Supplementary Fig. 1a, Supplementary data 1**). In the second group with the

## Molecular impact of electrical stimulation

123 unstimulated paradigm (4 participants), a sample was taken at baseline, and then a  
124 second sample was taken without stimulation about 30 minutes later ( $37.3 \pm 12.5$  mins,  
125 **Fig. 1b; Supplementary Fig. 1a**). The pre-stimulation sample and the unstimulated  
126 paradigm groups serves as controls for changes in baseline gene expression and  
127 changes in gene expression occurring as a result of the surgical procedure. Among the  
128 8 participants, five were under general anesthesia, whereas three participants were  
129 awake during the surgical procedure. All the resected tissue samples from both the  
130 stimulated and unstimulated paradigms were taken well outside the seizure focus ( $27.8$   
131  $\pm 7$ mm from the border of seizure focus, **Supplementary Fig. 1b**).

132 Tissue samples were first subjected to bulk whole-transcriptome RNA sequencing  
133 (RNA-seq) to identify differentially expressed genes following electrical stimulation. Bulk  
134 RNA-seq analysis from the stimulated and corresponding baseline samples revealed  
135 124 differentially expressed genes following electrical stimulation, with 112 up-regulated  
136 and 12 down-regulated genes (**Fig. 1c; Supplementary data 2**). Enrichment network  
137 analysis was used to identify the pathways most represented among the differentially  
138 expressed genes in the stimulated paradigm. The top significant pathways were  
139 enriched with genes involved in cytokine activity, DNA-binding transcription activator  
140 activity (RNA Pol II), cytokine receptor binding, DNA-binding transcription activator  
141 activity, nuclear glucocorticoid receptor binding, chemokine activity, CCR chemokine  
142 receptor binding, RNA pol II specific DNA binding, chemokine receptor binding, and  
143 protein phosphatase activity (**Fig. 1d**). Notably, these genes were not significantly  
144 enriched for previously identified genes induced in regions showing seizure activity in  
145 the human brain (**Supplementary Fig. 2**)<sup>26</sup>.

146 Bulk RNA-seq analysis from the unstimulated paradigm comparing unstimulated  
147 samples with corresponding baseline samples identified differential expression of only  
148 16 genes, with nine up-regulated and seven down-regulated genes (**Fig. 1e,**  
149 **Supplementary data 3**). Only one gene, *NR4A3*, was found to be differentially  
150 expressed in both the stimulated and unstimulated groups (**Fig. 1g**). The lack of overlap  
151 between the differentially expressed genes observed in our stimulated and unstimulated  
152 groups suggests that the changes in gene expression that we see following electrical

## Molecular impact of electrical stimulation

153 stimulation do not reflect disease state or surgical effects such as craniotomy, brain  
154 temperature, and anesthesia, but reflect changes due to electrical stimulation.

155 We used a similar electrical stimulation paradigm in the mouse non-primary auditory  
156 cortex to investigate whether these gene expression changes are unique to human  
157 samples and to determine whether they are related to disease state<sup>26,27</sup>. Bulk RNA-seq  
158 was performed from samples collected 30 minutes following electrical stimulation and  
159 unstimulated samples collected at the same time from the contralateral side (**Fig. 2a**).  
160 Bulk RNA-seq identified 44 upregulated and 107 downregulated genes (**Fig. 2b**,  
161 **Supplementary data 4**). Pathway analysis identified from the upregulated genes were  
162 enriched for cytokine activity, chemokine activity, cytokine receptor binding, and CCR  
163 chemokine receptor binding. (**Fig. 2c**). We also found upregulated pathways linked to  
164 transcription and post-transcription regulatory pathways, such as mRNA 3'-UTR binding,  
165 mRNA3'-UTR AU-rich region binding, and transcription co-repressor activity. Comparing  
166 the stimulation-responsive genes from human bulk RNA-seq and mouse bulk RNA-seq  
167 revealed a significant correlation ( $R^2=0.0415$ , p-value  $<0.00001$ ), especially cytokine-  
168 related genes were commonly upregulated following electrical stimulation in both  
169 humans and mice (**Fig. 2d**). Some of the pathways commonly altered by electrical  
170 stimulation between humans and mice are cytokine activity, chemokine activity,  
171 chemokine receptor binding, cytokine receptor activity, and the CCR chemokine  
172 receptor binding. Some common genes enriched in these chemokine and cytokine-  
173 related pathways are *CCL3*, *CCL4*, *CXCL1*, *IL1A*, and *TNF*. We further validated the  
174 expression of the cytokine activity-related genes *Ccl3* and *Ccl4* using qPCR analysis  
175 from mouse brain following electrical stimulation (**Fig. 2e**). The differentially expressed  
176 genes following electrical stimulation in the human cortex correlated significantly with  
177 learning-induced genes in the mouse cortex ( $R^2=0.2027$ , p-value  $<0.00001$ ). Immediate  
178 early genes such as *Arc*, *Fos*, *Egr1*, *Nr4a1*, and *FosB* were upregulated in both  
179 datasets (**Supplementary Fig. 3**). However, learning did not induce expression of  
180 cytokine activity related genes in mouse cortex. Thus, our findings of gene expression  
181 signature in response to electrical stimulation in the human and mouse brain reveal a  
182 molecular signature that partially conserved across species.

## Molecular impact of electrical stimulation

183 Next, we investigated the cell types exhibiting differential gene expression following  
184 electrical stimulation in the human brain by utilizing single nuclei multiomics (RNA and  
185 ATAC) on samples from the stimulated paradigm from 3 participants (**Fig 3a,**  
186 **Supplementary Fig. 4**). Cell clustering analysis identified seven major cell types in our  
187 samples—excitatory neurons, microglia, VIP-Sncg-Lamp5 inhibitory neurons, PValb-Sst  
188 inhibitory neurons, oligodendrocytes, oligodendrocytes precursor cells (OPC), and  
189 astrocytes (**Fig. 3b**). To determine the differentially expressed genes in each cell type  
190 following electrical stimulation, we performed a pseudobulk RNA-seq analysis due to its  
191 superior performance for detecting differential expression in single-cell RNA-sequencing  
192 analyses<sup>28</sup> and the stringent nature of this analysis. The pseudobulk analysis revealed  
193 that the microglia displayed the highest differential gene expression of all cell types with  
194 31 upregulated genes (**Fig. 3c, Supplementary data 5**). Genes related to cytokine  
195 activity (*CCL3*, *CCL4*, *CCL3L1*, and *IL1B*,) were upregulated exclusively within  
196 microglia. Five genes were upregulated in oligodendrocytes (*FOS*, *HSPA1A*, *JUNB*,  
197 *GADD45B*, and *FOSB*), and only two genes were differentially expressed (one  
198 upregulated: *LHFPL3*, and one downregulated: *ROBO2*) in astrocytes (**Supplementary**  
199 **data 5**). Surprisingly, no differentially expressed genes were detected within the  
200 neuronal cell types (excitatory and inhibitory neuronal cell types). Comparing the  
201 upregulated genes in microglia with human and mice bulk RNA seq revealed 5 genes  
202 (*Fos*, *Dusp1*, *Ccl3*, *Ccl4*, *Zfp36*) that are commonly upregulated following electrical  
203 stimulation (**Fig. 3d**). *Atf3*, *Cd83*, *Egr3*, *Nr4a1*, *Il1b*, *Mcl1*, *Nedd9*, *Spp1*, *Nfkbid*, *Rgs1*,  
204 and *Ccl3l1* were found to be human microglia-specific genes induced by electrical  
205 stimulation that do not change in the mice cortex (**Fig 3d**). Pathways enriched among  
206 the upregulated genes in microglia included cytokine-related pathways such as cytokine  
207 activity, chemokine activity, CCR chemokine receptor, and cytokine receptor binding  
208 (**Fig. 3e**). Microglia exhibited activation of transcription regulatory pathways such as  
209 DNA-binding transcription activator activity and RNA polymerase-specific DNA binding  
210 TF binding (**Fig. 3e**). These results reveal that electrical stimulation increases the  
211 expression of genes that are involved in cytokine activity and transcription regulation in  
212 microglia.



## Molecular impact of electrical stimulation

213 To investigate if electrical stimulation has an impact on the epigenome, we assessed  
214 chromatin accessibility using the single nuclear assay for transposase-accessible  
215 chromatin with sequencing (snATAC-seq)<sup>29</sup> on human samples from the stimulated  
216 paradigm. We focused on promoter accessibility (-2 to +2 kb from TSS) to analyze  
217 changes in chromatin accessibility in snATAC-seq data (**Supplementary data 6**). The  
218 differentially accessible regions that were either enriched or depleted following electrical  
219 stimulation in microglia significantly correlated ( $R^2=0.0262$ ,  $p\text{-value}<0.002$ ) with the  
220 microglia gene expression from snRNA-seq (**Fig. 3f**), suggesting that the genes that  
221 exhibit induced expression following electrical stimulation also exhibit increased  
222 chromatin accessibility. Genes related to transcription regulators, such as NR4A1 and  
223 FOS, showed a positive correlation between transcriptome and chromatin accessibility.  
224 We also found enriched promoter accessibility and increased gene expression for CCL4  
225 in microglia following electrical stimulation (**Fig 3g**). A recent study demonstrated that  
226 ambient RNA from neurons may contaminate non-neuronal cells in single-nuclei  
227 transcriptomic data<sup>30</sup>. Our snRNA seq data revealed the upregulation of several IEGs,  
228 such as *FOS*, *EGR3*, *JUNB*, and *NR4A1* within microglia. These genes are often seen  
229 to be upregulated in neurons following neuronal activation. However, our snATAC-seq  
230 data from the same samples also showed increased chromatin accessibility in microglial  
231 populations within IEG promoters, thus suggesting that the microglia-specific IEG  
232 expression is not due to neuronal ambient RNA contamination. Lastly, we analyzed  
233 genome-wide transcription factor (TF) binding motifs from the upregulated peaks  
234 following electrical stimulation in microglia using chromatin accessibility data.  
235 Genomewide TF motif analysis revealed enrichment of binding motifs for ELK3, ELK1,  
236 YY2, NRF1, HINFP, and ELK4 (**Fig. 3h, Supplementary data 7**). Interestingly, ELK4, a  
237 transcription factor downstream of MAPK signaling, is predicted to positively regulate  
238 the expression of *Ccl3* and *Ccl4*<sup>31</sup>. Thus, our sn-ATAC-seq results reveal a signature of  
239 transcription factor motifs and chromatin accessibility underlying electrical stimulation-  
240 induced gene expression in human microglia.

241 Our experimental design included internal controls (baseline/unstimulated samples)  
242 from each participant, enabling us to investigate the impact of electrical stimulation  
243 across individual participants. Therefore, we next examined the cell type-specific



## Molecular impact of electrical stimulation

244 response to electrical stimulation from within participants using our newly developed  
245 deep-learning computational tool, NEUROeSTIMator<sup>32</sup>, to map the active population of  
246 cells following electrical stimulation in each participant, comparing stimulated samples  
247 with corresponding baseline controls. We estimated cell activity from the single nuclei  
248 RNA data from individual populations of cells with either baseline or stimulated from  
249 each participants (**Fig. 4a**). We used paired linear regression with bootstrap sampling to  
250 assess differences in estimated activity between conditions for each cell type (**Fig. 4b**).  
251 Interestingly, we observed that the microglial cluster showed a significant increase in  
252 activity scores following stimulation, and this effect was consistent across all three  
253 participants [ $\beta = 0.100301$ , p-value <  $2e-16$ ] (**Fig. 4c**). This data supports our bulk RNA  
254 seq and snRNAseq data. However, we observed variability in electrical stimulation-  
255 mediated activation of excitatory neurons across participants. We detected significant  
256 differences in activity when using all three participants [ $\beta = -0.053920$ , p-value <  $2e-16$ ].  
257 One pair of samples showed a significant increase in activity [ $\beta = 0.032528$ , p-value =  
258  $0.000807$ ], while 2 out of 3 pairs showed a significant decrease in activity [ $\beta = -$   
259  $0.022086$ ,  $-0.083254$ , p-values =  $1.58e-8$ ,  $4e-9$ ] (**Fig. 4c**). Variability in activity estimates  
260 was also observed in inhibitory neuronal sub-types across participants (**Fig. 4c**).

261 To further investigate the epigenomic signature of cellular activity following electrical  
262 stimulation, we estimated activity from snATAC-seq data using a similar approach (**Fig.**  
263 **5a**). Activity was estimated for cells using gene-level counts in promoter regions and  
264 paired linear regression with bootstrap sampling was used to assess activity between  
265 baseline and electrical stimulation (**Fig. 5b**). Consistent with the transcriptomics data,  
266 microglia showed a significant increase in promoter-informed activity estimates, and this  
267 effect was consistent across all three participants [ $\beta = 0.060977$ , p-value <  $2e-16$ ] (**Fig.**  
268 **5c**). Neuronal clusters showed variability in activation in activity when considering all  
269 three participants [ $\beta_{\text{Excitatory}} = 0.016163$ , p-value<sub>Excitatory</sub> =  $0.000247$ ;  $\beta_{\text{Inhibitory}} = 0.028302$ ,  
270 p-value<sub>Inhibitory</sub> =  $2.283e-7$ ]. Only one participant showed a significant increase in the  
271 excitatory [ $\beta = 0.04712$ , p-val =  $0.000314$ ] and inhibitory neurons (Sst-Pvalb) [ $\beta =$   
272  $0.08863$ , p-value =  $0.00201$ ]. These findings suggest that microglia exhibit robust  
273 transcriptional and epigenomic responses to electrical stimulation and that neuronal cell  
274 types exhibit greater variability between patient participants.

275 **Discussion**

276 Electrical stimulation is a model for studying the human cortex with protocols that are  
277 used clinically for mapping the function of specific brain regions. Here, we take a  
278 molecular approach, defining the transcriptomic and epigenomic signatures of electrical  
279 stimulation at the single cell level in the human cortex in neurosurgical patient  
280 participants. Researchers have correlated human brain transcriptomics with prior  
281 recorded oscillatory signatures of memory consolidation<sup>22,33</sup>, but have not previously  
282 examined the changes in gene expression that are rapidly and directly driven by  
283 electrical stimulation. Most work thus far has emphasized the role of neurons in  
284 responding to external stimuli, but our work reveals the critical role of microglia in  
285 sculpting the activity and function of brain circuits. In microglia, genes related to  
286 cytokine signaling showed the greatest induction pattern, and this was conserved  
287 across species. As previously hypothesized, we observed the induction of activity-  
288 dependent genes in our bulk RNA sequencing results, but to our surprise, single nuclei  
289 multiomics experiments revealed pronounced microglia-specific transcriptomic  
290 activation following electrical stimulation that was supported by analysis using  
291 NEUROeSTIMator<sup>32</sup>, a deep-learning computational model. Identifying a microglial  
292 transcriptomic response following electrical stimulation represents an important  
293 conceptual advance in our understanding of the impact of this common form of electrical  
294 stimulation used clinically.

295 Microglia are critical modulators of neuronal function, acting to suppress excessive  
296 activity by inhibiting surrounding neurons, including excitatory neurons<sup>34</sup>. Although  
297 classified as non-excitabile cells, microglia exhibit electrophysiological stimulus-  
298 response features, and changes in their membrane potential affect crucial microglial  
299 functions including phagocytosis, chemotaxis, and cytokine release<sup>35</sup>. Our analyses  
300 identified critical molecular components within microglia that change with electrical  
301 stimulation, including chemokine-encoding genes such as *CCL3* and *CCL4*, which act to  
302 alter microglial motility, influence neuronal-microglial interactions, and shape neuronal  
303 connectivity<sup>34,36-39</sup>. These chemokines are ligands for C-C chemokine receptor type 5  
304 (CCR5), which regulates neuronal excitability and memory allocation in the  
305 hippocampus<sup>40</sup>. Previous rodent studies have shown that neuronal activation using

## Molecular impact of electrical stimulation

306 chemogenetic approaches leads to distinct gene expression changes in microglia,  
307 including genes encoding chemokines<sup>34</sup>. Our work also revealed that genes encoding  
308 transcription factors such as FOS and NR4A1 are induced in microglia in response to  
309 electrical stimulation. Further, we observed increased promoter accessibility at these  
310 genes, underscoring the conclusion that these genes are transcriptionally upregulated in  
311 microglia after stimulation and broadening the potential functional impact of these  
312 immediate early genes beyond their more frequently studied role in neurons. Indeed,  
313 NR4A1 acts in neurons as a transcription factor essential for memory consolidation<sup>41,42</sup>  
314 and functions in microglia as a molecular rheostat, contributing to the maintenance of a  
315 threshold that prevents microglial activation<sup>43</sup>. Furthermore, our study of chromatin  
316 accessibility defines a cell-type-specific signature of transcriptional motifs driving these  
317 processes that includes motifs for ELK4 and NRF1, which have been identified in other  
318 studies as transcriptional motifs associated with the differential regulation of molecular  
319 pathways in specific subsets of microglia<sup>44,45</sup>.

320 This study represents a rare opportunity to define the molecular impact of electrical  
321 stimulation in patients undergoing anterior temporal lobectomy due to therapy refractory  
322 seizures. Although presenting a unique opportunity, it is important to note the caveats  
323 that come from this research carried out in a setting focused on clinical efficacy in  
324 patients that have epilepsy. Thus, we can not control all of the parameters as we might  
325 in an experiment carried out in a model organism, although we have worked to address  
326 three potential limitations of our study. First, our experimental design includes a group  
327 that does not receive electrical stimulation, thus controlling for the impact of the surgical  
328 procedure, craniotomy, brain temperature changes, and levels of anesthesia when  
329 present. We also show that electrical stimulation in a mouse model, in which we can  
330 control many additional parameters, gives rise to similar molecular changes.  
331 Importantly, our mouse experiment included the use of an inactive electrode, thus  
332 controlling for mechanically induced changes in gene expression. Second, the  
333 stimulation pattern used is safe and efficacious for brain mapping in human patients but  
334 is not optimized to modulate activity in specific circuits and cell types in the brain.  
335 Indeed, the stimulation protocol used leads to the functional disruption of brain regions<sup>1</sup>,  
336 and thus, we may expect to see reductions in activity-dependent gene expression in

## Molecular impact of electrical stimulation

337 excitatory neurons, as seen in two patients in our NEUROeSTIMator analysis. Third, it  
338 goes without saying that these patients have severe therapy refractory epilepsy.  
339 However, the resected samples were taken a considerable distance from the seizure  
340 foci (see Suppl. Fig. 1b), our gene induction signatures do not resemble those seen in  
341 actively spiking tissue<sup>26</sup>, and our molecular changes are seen in a mouse model that  
342 does not exhibit seizures.

343 Despite these caveats, we were able to identify a reliable cell-specific signature of the  
344 impact of electrical stimulation in the living human brain. This study demonstrates for the  
345 first time a unique transcriptomic and epigenomic signature in microglia following direct  
346 electrical stimulation, representing a conceptual advance in our understanding of how  
347 the brain responds to an important clinical tool used to map brain function. These  
348 findings have the potential to inform the clinical practice of diagnostic and therapeutic  
349 brain stimulation. Clinical and translational research has focused mainly on the  
350 immediate effects of stimulation in neuronal populations, while microglia receive little  
351 attention, often being discussed with regard to neuroimmunological aspects<sup>46</sup>. Although,  
352 for clinical mapping, clinicians rely on the immediate neuronal effects on behavior (e.g.,  
353 speech arrest), there is growing evidence that therapeutic effects of electrical  
354 stimulation can accumulate gradually over time<sup>47</sup>. We could not test a range of  
355 stimulation frequencies and intensities or examine a broad range of brain areas  
356 because of clinical limitations, but our results raise the intriguing hypothesis that  
357 microglia, not just neurons, shape plasticity after repetitive stimulation. Our work further  
358 highlights that cytokine and chemokine-based mechanisms enable microglia to respond  
359 to electrical stimulation and sculpt circuit function, making these potential targets to  
360 modify circuit activity with pharmacological approaches. Microglia exist in different  
361 subpopulations depending on transcriptional state and age<sup>48,49</sup>, and our epigenetic work  
362 has revealed particular transcriptional motifs that mark microglial subtypes important for  
363 cortical plasticity. It will be especially interesting in future work to extend our studies to  
364 stimulation protocols used therapeutically as well as natural stimuli to probe the critical  
365 role of microglial signaling in mediating the response of the human brain to experience.

## 366 **Acknowledgments**

## Molecular impact of electrical stimulation

367 We thank Rashmi N. Mueller who oversaw anesthesia to manage pain levels before,  
368 during, and after surgical procedures, and Kyle S. Conway for helping with the initial  
369 pathological assessment. We thank the Iowa Institute of Human Genetics (IIHG) core  
370 for RNA seq library preparation and sequencing.

371 **Funding:** This work was supported by grants from the National Institute of Health R01  
372 MH 087463 to T.A and The University of Iowa Hawkeye Intellectual and Developmental  
373 Disabilities Research Center (HAWK-IDDRC) P50 HD103556 to T.A., The National  
374 Institute of Health R00 AG068306 to S.C. and the National Institute of Health R01  
375 DC004290 to M.A.H., National Science Foundation BCS-2342847 to C.I.P. T.N.J &  
376 C.I.P. are supported by a Research Program of Excellence of the Carver Trust and the  
377 Iowa Neuroscience Institute. T.A. is supported by the Roy J. Carver Chair of  
378 Neuroscience, JMM is supported by the Roy J. Carver Professor of Neuroscience and  
379 the Andrew H. Woods Professorship supported T.N.J. The Neural Circuits and Behavior  
380 Core as well as the NeuroBank Core are supported by the Roy J. Carver Charitable  
381 Trust.

### 382 **Author contributions**

383 S.C., M.A.H., and T.A. conceived the project, designed the experiments, and interpreted  
384 the data. S.C. and T.A. wrote the manuscript with assistance from C.I.P., L.L., and  
385 T.N.J., and inputs from other co-authors. H.K. performed human surgery and electrical  
386 stimulation and resected the tissue. A.E.R and C.K.K. processed with IRB and MRI  
387 imaging registration. H.O, M.A.H, T.N-J, and K.V.L provided advice on surgical  
388 procedures and electrical stimulation. M.M.H. provided a pathological assessment.  
389 L.C.L., K.V.N., and B.J.P. collected the tissue and images during resection. S.C., B.J.P.,  
390 L.C.L., U.M., L.L. performed human or mouse tissue samples experiments. C.I.P. and  
391 Y.A.A. performed distance to the seizure site analysis. U.M. and L.L. performed mouse  
392 brain imaging and data analysis. Y.V., A.I.G., and B.B. performed the bioinformatics  
393 analysis with inputs from E.B. and J.J.M. S.A.H. performed the mouse surgery and  
394 electrical stimulation experiments. K.V.N, C.K.K, Z.K. Y.K, C.I.P, M.H, J.J.M, E.B, U.M,  
395 and T.N.J. provided input on data analysis and interpretation. All authors discussed the  
396 results and commented on the manuscript.

397 **Competing interests**

398 T.A. is a scientific advisor to Aditum Bio and Radius Health and serves on the scientific  
399 advisory board of Embark Neuro. The other authors declare no conflicting interests.

400 **Figure legends**

401 **Figure 1. Electrical stimulation of the human cortex induces changes in genes**  
402 **associated with cytokine activity and transcription regulation. a, b.** Schematics of  
403 stimulated (**a**) and unstimulated (**b**) paradigms in the human anterior temporal lobe. For  
404 both paradigms sample A was taken at  $T = 0$  minutes then an adjacent sample B was  
405 taken at either 30 min after stimulation (**a**, stimulated paradigm, 4 participants) or 30 min  
406 after sample A was taken (**b**, unstimulated paradigm, 4 participants). **c.** Volcano plot  
407 showing gene expression changes in the stimulated samples. The most significant  
408 genes ( $FDR < 0.05$ ) are labeled in red (upregulated) or blue (downregulated). **d.** Cnet  
409 plot showing pathway enrichment analysis of the genes significantly ( $FDR < 0.05$ )  
410 differentially expressed in the stimulated samples. **e.** Volcano plots showing gene  
411 expression changes in the unstimulated samples. The most significant genes ( $FDR <$   
412  $0.05$ ) are labeled in red (upregulated) or blue (downregulated).

413 **Figure 2. Electrical stimulation of mouse cortex induces changes in genes**  
414 **associated with cytokine activity and transcription regulation. a.** The mouse  
415 auditory cortex was stimulated, tissue was collected 30 min later, and the contralateral  
416 auditory cortex was obtained as baseline control. **b.** Volcano plot showing gene  
417 expression changes after stimulation. The most significant genes ( $FDR < 0.05$ ) are  
418 labeled in red (upregulated) or blue (downregulated). **c.** Cnet plot showing pathway  
419 enrichment analysis of the genes significantly ( $FDR < 0.05$ ) affected by electrical  
420 stimulation. **d.** Quadrant plot comparing genes induced by electrical stimulation in mice  
421 with genes induced by electrical stimulation in human brain. Genes upregulated in both  
422 mice and human brains after stimulation are labeled. The size, opacity, and color  
423 intensity of each data point denotes the minimum false discovery rate value for a gene  
424 between each transcriptomic datasets. **e.** qPCR analysis of the genes related to  
425 cytokine activity comparing stimulated versus baseline controls in mice cortex.  
426  $n=7$ /group.



## Molecular impact of electrical stimulation

427 **Figure 3. Single nuclei multiomics reveal cell type-specific transcriptomic and**  
428 **epigenomic changes following electrical stimulation. a.** Single nucleus multiomic  
429 experimental approach. **b.** UMAP shows the specific cell types from each cluster. **c.**  
430 Volcano plot showing differentially expressed genes in microglia using pseudobulk  
431 analysis comparing stimulated vs baseline samples from human brain (FDR<0.1). **d.**  
432 Upset plot comparing DEGs in mouse, human bulk RNA seq, and human microglia  
433 snRNA-seq after electrical stimulation. **e.** Cnet plot showing pathway enrichment  
434 analysis of the genes significantly (FDR < 0.1) affected by electrical stimulation in  
435 human microglia. **f.** Quadrant plot comparing DEGs from snRNA-seq following  
436 electrical stimulation in human microglia and genes with open chromatin accessibility  
437 from snATAC-seq in microglia following electrical stimulation. Genes upregulated in both  
438 mice and human brains after stimulation are labeled. **g.** Quadrant plot comparing gene  
439 expression changes ( $\log_{10}(\text{FDR}) \times \log_2(\text{fold-change})$ ) between snRNA-seq (x-axis) and  
440 snATAC-seq (y-axis) data in microglia after stimulation. Genes in red in the top-right  
441 corner of the plot are significantly upregulated at the gene expression level and exhibit  
442 increased chromatin accessibility. The dotted lines represent FDR thresholds of 0.01.  
443 The dashed line represents the linear regression applied to this quadrant plot. **g.** DNA  
444 motifs are overrepresented in the set of peaks differentially accessible in microglia after  
445 stimulation. Motifs are ranked based on significance from the most significant left to  
446 right. **h.** The coverage plot shows ATAC peaks at the CCL4 locus. Each track represents  
447 a normalized chromatin accessibility signal from the ATAC assay for each cell type and  
448 condition (baseline or stimulated).

449 **Figure 4. NEUROeSTIMator for snRNA-seq. Cell-type specific differences in**  
450 **activity estimates. a.** UMAP of cells representing the activity estimated from the RNA  
451 gene counts in the baseline and stimulated conditions. Darker blue points are cells with  
452 higher estimated activity. **b.** The bootstrap distribution of the difference between activity  
453 estimates (stimulated – baseline) by cell type. Horizontal bars indicate the 95%  
454 confidence interval of the mean difference in activity estimate. **c.** Activity estimates in  
455 selected cell types in baseline (green) and stimulated (orange) conditions.

456 **Figure 5. NEUROeSTIMator for snATAC-seq. Cell-type specific differences in**  
457 **activity estimates. a.** UMAP of cells representing the activity estimated from the ATAC

## Molecular impact of electrical stimulation

458 counts in the baseline and stimulated conditions. Darker blue points are cells with  
459 higher estimated activity. **b.** The bootstrap distribution of the difference between activity  
460 estimates (stimulated – baseline) by cell type. Horizontal bars indicate the 95%  
461 confidence interval of the mean difference in activity estimate. **c.** Activity estimates in  
462 selected cell types in baseline (green) and stimulated (orange) conditions.

### 463 **Materials and Methods:**

464 ***Patient participants:*** The study participants were 8 adult neurosurgical patients (6  
465 female, 2 male, age 19-63 years old, median age 41 years old) with medically refractory  
466 epilepsy. The patients were undergoing surgical resection of seizure foci following non-  
467 invasive electroencephalography (EEG) or invasive iEEG monitoring. All patients were  
468 diagnosed with intractable epilepsy. All patients underwent ATL resection surgery for  
469 epilepsy of various etiologies (**Extended data fig 1**).

470 Two of the patient participants, L472 had a cavernoma and L475 had a  
471 dysembryoplastic neuroepithelial tumor. X out of Y participants were required to be  
472 awake during the surgical resection, and the rest were anesthetized. All patient  
473 participants except #6 were non-smokers. Participant's age, sex, surgery, and awake or  
474 sedative information were recorded (**Extended Data Table 1**). All participants were  
475 native English speakers, 7 were right-handed, 1 was left-handed, and all had left  
476 language dominance as determined by Wada tests. All participants underwent  
477 audiometric evaluation before the study, and none were found to have hearing deficits  
478 or word recognition scores deemed sufficient to affect the findings presented in this  
479 study. The vision was self-reported as normal or corrected to normal with glasses or  
480 contact lenses. As determined by standard neuropsychological assessments, cognitive  
481 function was in the average range in all participants. Research protocols were  
482 approved by the University of Iowa Institutional Review Board (IRB 201910791,  
483 201911084) and the National Institutes of Health. Written informed consent was  
484 obtained from all participants.

485 ***Procedure:*** Surgery was performed awake, under general anesthesia or monitored  
486 anesthetic care. Standard craniotomy was performed by the same senior epilepsy  
487 neurosurgeon in all patients to reach the epilepsy focus for resection, which involved the

## Molecular impact of electrical stimulation

488 anterior and medial temporal lobe in all patients except one who had a temporal  
489 encephalocele and surrounding anterolateral temporal cortical focus. Before  
490 neurosurgical ATL resection, cortical tissue from the anterior temporal lobe was sampled  
491 by the neurosurgeon and handed over to the research team for analysis. The  
492 experimental condition was defined by an electrical “stimulation paradigm” and a control  
493 “no-stimulation paradigm”. The location of the sampled tissue is plotted on anatomic  
494 brain reconstructions (**Extended data fig 1**). The 30 minutes in between the control and  
495 experimental samples was clinically required for the clinical EEG team to record inter-  
496 ictal activity with surface recording grids placed gently on the brain surface.

497 There were 4 participants (1 iEEG and 3 EEG patients) who underwent the “stimulation  
498 paradigm” and 4 (2 iEEG and 2 EEG patients) who underwent the “no-stimulation  
499 paradigm” (**Extended Data Table 5**).

500 In the “stimulation paradigm”, a baseline sample was obtained from the anterior  
501 temporal cortex that would be resected in the planned surgical resection. The area  
502 directly adjacent to where the baseline sample was collected was stimulated with direct  
503 bipolar electric stimulation (50 Hz frequency, 0.2 ms pulse duration, 2 min stimulation  
504 duration, and 10 V voltage). The stimulated area was then sampled after a period of 30  
505 minutes to allow for gene expression<sup>50,51</sup>. In the “no stimulation paradigm”, no direct  
506 electric stimulation was performed and the area directly adjacent to the baseline sample  
507 was collected 30 minutes after initial baseline sampling.

508 After sampling the tissue samples were immediately placed in a sterile container on dry  
509 ice. The average weight of the baseline sample was  $88.0 \pm 33.2$  mg (mean, standard  
510 deviation) and the adjacent sample was  $113.4 \pm 62.7$  mg. After the collection of all  
511 samples in this fashion, they were weighed and transferred to a freezer at  $-80^{\circ}$  C for  
512 storage until further testing.

513 **Sample Localization to MNI space:** All samples were from the same cortical region.  
514 Intraoperative photos of the sample sites were obtained during the time of surgery.  
515 Using patient participant matched preoperative T1 sequence MRI, the sample sites  
516 were mapped onto their anatomic brain reconstructions (**Extended data fig. 1**). They  
517 were also mapped onto MNI space coordinates.

## Molecular impact of electrical stimulation

518 **Human cortical tissue RNA extraction, library preparation, and sequencing:** Total  
519 RNA was extracted from sampled human brains using miRNeasy Mini Kit (Qiagen, CA,  
520 USA). The tissue samples were homogenized in QIAzol (Qiagen, CA, USA)  
521 stainless steel beads (Qiagen, CA, USA). Chloroform was then used for phase  
522 separation. RNA containing an aqueous layer was further purified using the  
523 RNeasy MinElute spin column. RNA was finally eluted in RNase-free water. RNA  
524 concentrations were estimated using a Nanodrop (Thermo Fisher Scientific, MA,  
525 USA) and Qubit (Thermo Fisher Scientific, MA, USA). RNA libraries were prepared at  
526 the Iowa Institute of Human Genetics (IIHG), Genomics Division, using the Illumina  
527 Stranded Total RNA Prep, Ligation with Ribo-Zero Plus (Illumina Inc., San Diego, CA).  
528 The KAPA Illumina Library Quantification Kit (KAPA Biosystems, Wilmington, MA) was  
529 used to measure library concentrations. Pooled libraries were sequenced on Illumina  
530 NovaSeq6000 sequencers with 150-bp paired-end chemistry (Illumina) at the Iowa  
531 Institute of Human Genetics (IIHG) core.

532 **Bulk RNA sequencing analysis:** RNA-seq data were processed with the bcbio-  
533 nextgen pipeline (<https://github.com/bcbio/bcbio-nextgen>, version 1.2.9). The pipeline  
534 uses STAR<sup>52</sup> to align reads to the hg38 or mm10 reference genome and quantifies  
535 expression at the gene level with feature Counts<sup>53</sup>. All further analyses were performed  
536 using R. For gene-level count data, the R package EDASeq was used to account for  
537 sequencing depth (upper quartile normalization)<sup>54</sup>. Latent sources of variation in  
538 expression levels were assessed and accounted for using RUVSeq (RUVs mode using  
539 all features)<sup>55</sup>. Appropriate choice of the RUVSeq parameter k was guided through  
540 inspection of principal components analysis (PCA) plots. Specifically, the smallest value  
541 k was chosen where PCA plots demonstrated replicate sample clustering in the first  
542 three principal components<sup>56</sup>. Differential expression analysis was conducted using the  
543 edgeR package<sup>57</sup>. Codes to reproduce the RNA-seq differential gene expression  
544 analysis are available at <https://github.com/YannVRB/Human-brain-stimulation.git>.

545 All the transcriptomics data have been deposited in NCBI's Gene Expression Omnibus  
546 and are accessible through GEO Series accession number [GSE224952](#).

547 **Downstream pathway analysis:**

## Molecular impact of electrical stimulation

548 The enrichment analysis of differentially expressed genes-associated pathways and  
549 molecular functions from the stimulated and unstimulated RNA-seq was performed with  
550 the Gene Ontology (GO–molecular function) databases using clusterProfiler package in  
551 R. Only the pathways with an adjusted p-value  $\leq 0.05$  were considered as significant  
552 and displayed. Further, the enrichment data were visualized using ‘cnetplot’ function of  
553 clusterProfiler.

554

555 ***Single-nuclei multiomics (nuclei isolation, library preparation, sequencing):*** Nuclei  
556 were isolated from brain tissue using the Chromium Nuclei Isolation Kit (10X  
557 Genomics). Briefly, frozen tissue was dissociated with pestle in lysis buffer, passed  
558 through nuclei isolation column and spun at 16,000 rcf for 20 sec at 4°C. Flowthrough  
559 was vortexed and spun at 500 rcf for 3 mins at 4°C. Pellet was resuspended with debris  
560 removal buffer and centrifuged at 700 rcf for 10 mins at 4°C, nuclei resuspended in  
561 wash buffer and centrifuged again at 500 rcf for 5 mins at 4°C. Pellet was resuspended  
562 in resuspension buffer and nuclei were counted using a hemocytometer. Nuclei were  
563 directly processed for droplet capture for single cell multiome ATAC + gene expression  
564 using a chromium controller (10X Genomics). Chromium Next GEM Single Cell  
565 Multiome ATAC + Gene v1 chemistry was used to create single nuclei ATAC and RNA  
566 libraries from the same cell. Two baseline and two stimulated samples were used for  
567 independent replicates. Libraries were sequenced on an Illumina Novaseq 6000 with a  
568 150 bp paired end read setup.

569 ***Single-nuclei multiomic data processing and analysis:*** To analyze the RNA part of  
570 the human brain stimulation multiomic data, gene counts were normalized and log  
571 transformed (LogNormalize), and the top 2,000 most variable features between each  
572 nuclei were identified using FindVariableFeatures (selection.method = ‘vst’). Features  
573 that are repeatedly variable across nuclei and datasets were selected for integration  
574 (SelectIntegrationFeatures). We then identified anchors (FindIntegrationAnchors), which  
575 took the list of 4 individual Seurat objects for each sample as input and used these  
576 anchors to integrate the four datasets together (IntegrateData). The following analyses  
577 were performed on the integrated Seurat object. Linear dimensionality reduction was

## Molecular impact of electrical stimulation

578 performed by principal component analysis (runPCA,  $npcs = 25$ ). A k-nearest-  
579 neighbors graph was constructed based on Euclidean distance in PCA space and  
580 refined (FindNeighbors,  $npcs = 30$ ), then nuclei were clustered using the Louvain  
581 algorithm (FindClusters,  $resolution = 0.5$ ). Clusters were visualized with UMAP  
582 (runUMAP,  $dims = 30$ ). Cell types were annotated by label transfer cell labels from an  
583 existing human primary motor cortex reference dataset from the Allen Institute (doi:  
584 [10.1038/s41586-021-03465-8](https://doi.org/10.1038/s41586-021-03465-8)) (FindTransferAnchors and TransferData). Cell types  
585 identification was validated by expression of specific biomarkers. Prior of running  
586 differential gene expression analysis, as recommended by recent publications  
587 (<https://doi.org/10.1038/nmeth.4612> and <https://doi.org/10.1038/s41467-020-19894-4>),  
588 we used an aggregation-based (pseudobulk) workflow. We aggregated all cells within  
589 the same cell type and sample using the AggregateExpression function. This returns a  
590 Seurat object where each 'cell' represents the pseudobulk profile of one cell type in one  
591 individual. After we aggregated cells, we performed celltype-specific differential  
592 expression between stimulated and baseline samples using DESeq2.

593 To analyze ATAC part of the human brain stimulation multiomic data, prior to integrating  
594 the four Seurat object, the default assay was switched to ATAC, and peak calling was  
595 performed. Since the set of peaks identified by Cellranger often merges distinct peaks  
596 that are close together, creating a problem for motif enrichment analysis and peak-to-  
597 gene linkage, we identified a more accurate set of peaks by calling peaks using MACS2  
598 (CallPeaks) on all cells together. Peaks on nonstandard chromosomes and in genomic  
599 blacklist regions were removed (keepStandardChromosomes and subsetByOverlaps).  
600 Normalization was performed with a frequency-inverse document frequency  
601 normalization which normalizes across cells and peaks (RunTFIDF). Then, a feature  
602 selection was performed using all the peaks as input (FindTopFeatures). The  
603 dimensional reduction was performed on the TF-IDF normalized matrix with the  
604 selected peaks using a singular value decomposition (RunSVD). To mimic the open  
605 chromatin conformation of a gene, a gene activity matrix was calculated using a window  
606 of 1000bp before and after the transcription start site of each protein coding gene  
607 (GeneActivity). Differentially accessible transcription start sites in individual clusters  
608 between baseline and stimulated samples were calculated using a logistic regression



## Molecular impact of electrical stimulation

609 framework (FindMarkers, test.use = 'LR', latent.vars = 'nCount\_peaks', Padj < 0.05).  
610 Motif and transcription factor enrichment analysis for Microglia cluster was performed  
611 using FindMotifs on genome-wide all peaks assay of the Seurat object. The top six  
612 enriched motifs in microglia cluster are shown. Genomic locations of typical genes like  
613 CCL4 were presented (CoveragePlot). It also includes co-accessibility between peaks  
614 and transcription start site of genes. Codes to reproduce the multiomic data analysis are  
615 available at <https://github.com/YannVRB/Human-brain-stimulation.git>.

616 **NEUROeSTIMator analysis.** Gene-level counts for each cell were used as input for the  
617 NEUROeSTIMator model<sup>33</sup> to estimate transcriptional signatures of cell activity. Activity  
618 was also estimated for cells using gene-level counts in promoter regions from the ATAC  
619 assay. Estimated activity was assessed for significant differences between the baseline  
620 and stimulated conditions across the donors and cell types using paired linear  
621 regression. P-values were adjusted for multiple testing with the Benjamini-Hochberg  
622 correction. To account for variable sample sizes across cell types and participants,  
623 bootstrap resampling was performed (n = 100 cells per donor, replicates = 1000) for  
624 each cell type in each condition to generate a distribution of the mean difference in  
625 estimated activity between conditions.

626 To account for variation in sample size across cell types and participants, bootstrap  
627 resampling was performed (n = 100 cells per participant, replicates = 1000) for each  
628 cell type of the mean difference in estimated activity scores between conditions (mean  
629 stimulated – mean baseline). The distributions were analyzed by mean and 95%  
630 confidence interval.

631 **Animals:** Adult male C57BL/6J mice were purchased from The Jackson Laboratory  
632 were 3 to 4 months of age during experiments. All mice had free access to food and  
633 water; lights were maintained on a 12-hour light/12-hour dark cycle.

634 **Mouse electrical stimulation:** Stimulation experiments were performed in anesthetized  
635 adult male C57BL6/J mice. Anesthesia was induced with 5% isoflurane by inhalation  
636 and maintained at 1.8-2% for the duration of the experiment. The mouse was placed in  
637 a stereotax (Kopf) and a midline incision was made and the skin retracted to expose the  
638 temporal muscle bilaterally. The dorsal insertion of both temporal muscles was

## Molecular impact of electrical stimulation

639 removed, and the muscles retracted. A 2-3 mm craniotomy was made over area AuV  
640 (centered at 2.9 mm posterior, 4.2 mm lateral, 2.8 mm ventral from Bregma based on  
641 Paxinos atlas) bilaterally to expose the cortical surface and a small square of gel foam  
642 soaked in ACSF was applied on top of the dura to prevent it from dehydrating. For each  
643 mouse the side of electrical stimulation and sham stimulation were alternated, with the  
644 sham side serving as the baseline control for gene expression profiling. Electrical  
645 stimulation was delivered through a bipolar ball electrode constructed from two silver  
646 wires in which the uninsulated tips were melted under a butane flame (1 mm tip size, 2  
647 mm tip spacing). For both electrical and sham stimulations, the gel foam was removed  
648 and the electrode was gently lowered to make contact with the cortical surface. For  
649 electrical stimulation, a biphasic pulse train was then delivered for two minutes (8 mA,  
650 50 Hz, 200  $\mu$ s pulse width). For the sham stimulation no current was delivered but the  
651 electrode was left in place for 2 minutes. Following electrical or sham stimulation the  
652 electrode was slowly retracted, and the exposed dura was covered with gel foam.  
653 Selection for hemisphere was performed randomly, which resulted in the order of  
654 electrical and sham stimulation alternating from mouse to mouse. No more than 5  
655 minutes elapsed between electrical or sham stimulation of both sides. After both sides  
656 were stimulated (electrical or sham) the mouse was left in the stereotax under  
657 anesthesia for 30 minutes before euthanasia and tissue collection. Tissue samples were  
658 immediately stored at  $-80^{\circ}\text{C}$  in RNA later solution (Ambion).

659 ***RNA extraction, cDNA preparation and qPCRs from mouse auditory cortex:*** Tissue  
660 samples were homogenized in Qiazol (Qiagen) using stainless steel beads (Qiagen).  
661 Chloroform was added and centrifuged at 12,000g at room temperature for 15 min to  
662 separate RNA in the aqueous phase. RNA was precipitated in ethanol and cleared using  
663 RNeasy kit (Qiagen). RNA eluted in nuclease-free water was then treated with DNase  
664 (Qiagen) at room temperature for 25 min to remove genomic DNA. RNA was further  
665 precipitated in ethanol, sodium acetate (pH 5.2) and glycogen overnight at  $-20^{\circ}\text{C}$ . RNA  
666 was precipitated by centrifugation at 30,000g for 20 min, precipitate washed with 70%  
667 ethanol and the dried RNA pellet was resuspended in nuclease-free water. RNA  
668 concentration was measured using NanoDrop (Thermo Fisher Scientific). 1  $\mu$ g of RNA  
669 was used for complementary DNA (cDNA) preparation using the SuperScript IV First-

## Molecular impact of electrical stimulation

670 Strand Synthesis System (Ambion). Real-time reverse transcription polymerase chain  
671 reactions (RT-PCRs) were performed on the QuantStudio 7 Flex Real-Time PCR  
672 System (Applied Biosystems, Life Technologies). Data were normalized to  
673 housekeeping genes (*Tubulin*, *Pgk1*, and *Actin*), and  $2^{(-\Delta\Delta Ct)}$  method was used for gene  
674 expression analysis.

675 **Mouse cortex spatial transcriptomics analysis (Yann):** Spatial transcriptomics data  
676 were obtained from the Visium Spatial Gene Expression platform, as described  
677 previously<sup>42</sup>. This dataset provides comprehensive gene expression profiles across  
678 various brain regions, including the mouse cortex. To focus on the mouse auditory  
679 cortex, the closest homolog to the human anterior temporal lobe, we manually selected  
680 spatial spots from the Visium data corresponding to this brain region. This selection was  
681 based on anatomical landmarks and known spatial coordinates for the auditory cortex.  
682 For each of the 14 mice in the dataset, we subsetted the data to include only these  
683 selected spots, thereby isolating the gene expression profiles specifically from the  
684 auditory cortex.

685 The dataset of 14 mice was divided into two experimental conditions: 7 mice underwent  
686 Spatial Object Recognition after 1 hour (SOR-1h), while the other 7 mice were kept in  
687 their homecage environment without specific tasks. Based on the Visium spots data  
688 overlaying the mouse auditory cortex, differential gene expression analysis was  
689 performed to identify genes that were significantly differentially expressed between the  
690 SOR-1h and homecage conditions.

691 **Statistics:** For the qPCR analysis, the Wilcoxon matched pairs signed rank test and  
692 one sample Wilcoxon test was performed.

## 693 References

- 694 1 Penfield, W. & Rasmussen, T. Vocalization and arrest of speech. *Arch Neurol*  
695 *Psychiatry* **61**, 21-27 (1949).  
696 <https://doi.org/10.1001/archneurpsyc.1949.02310070027002>
- 697 2 Lozano, A. M. *et al.* Deep brain stimulation: current challenges and future  
698 directions. *Nat Rev Neurol* **15**, 148-160 (2019). [https://doi.org/10.1038/s41582-](https://doi.org/10.1038/s41582-018-0128-2)  
699 [018-0128-2](https://doi.org/10.1038/s41582-018-0128-2)

## Molecular impact of electrical stimulation

- 700 3 Okun, M. S. Deep-brain stimulation for Parkinson's disease. *N Engl J Med* **367**,  
701 1529-1538 (2012). <https://doi.org/10.1056/NEJMct1208070>
- 702 4 De Risio, L. *et al.* Recovering from depression with repetitive transcranial  
703 magnetic stimulation (rTMS): a systematic review and meta-analysis of  
704 preclinical studies. *Transl Psychiatry* **10**, 393 (2020).  
705 <https://doi.org/10.1038/s41398-020-01055-2>
- 706 5 Kellner, C. H. *et al.* ECT in treatment-resistant depression. *Am J Psychiatry* **169**,  
707 1238-1244 (2012). <https://doi.org/10.1176/appi.ajp.2012.12050648>
- 708 6 Krauss, J. K. *et al.* Technology of deep brain stimulation: current status and  
709 future directions. *Nat Rev Neurol* **17**, 75-87 (2021).  
710 <https://doi.org/10.1038/s41582-020-00426-z>
- 711 7 Sheth, S. A. & Mayberg, H. S. Deep Brain Stimulation for Obsessive-Compulsive  
712 Disorder and Depression. *Annu Rev Neurosci* **46**, 341-358 (2023).  
713 <https://doi.org/10.1146/annurev-neuro-110122-110434>
- 714 8 Goodman, W. K., Storch, E. A. & Sheth, S. A. Harmonizing the Neurobiology and  
715 Treatment of Obsessive-Compulsive Disorder. *Am J Psychiatry* **178**, 17-29  
716 (2021). <https://doi.org/10.1176/appi.ajp.2020.20111601>
- 717 9 George, D. D., Ojemann, S. G., Drees, C. & Thompson, J. A. Stimulation  
718 Mapping Using Stereoelectroencephalography: Current and Future Directions.  
719 *Front Neurol* **11**, 320 (2020). <https://doi.org/10.3389/fneur.2020.00320>
- 720 10 Grande, K. M., Ihnen, S. K. Z. & Arya, R. Electrical Stimulation Mapping of Brain  
721 Function: A Comparison of Subdural Electrodes and Stereo-EEG. *Front Hum*  
722 *Neurosci* **14**, 611291 (2020). <https://doi.org/10.3389/fnhum.2020.611291>
- 723 11 Yap, E. L. & Greenberg, M. E. Activity-Regulated Transcription: Bridging the Gap  
724 between Neural Activity and Behavior. *Neuron* **100**, 330-348 (2018).  
725 <https://doi.org/10.1016/j.neuron.2018.10.013>
- 726 12 Sagar, S. M., Sharp, F. R. & Curran, T. Expression of c-fos protein in brain:  
727 metabolic mapping at the cellular level. *Science* **240**, 1328-1331 (1988).  
728 <https://doi.org/10.1126/science.3131879>
- 729 13 Guzowski, J. F., McNaughton, B. L., Barnes, C. A. & Worley, P. F. Environment-  
730 specific expression of the immediate-early gene Arc in hippocampal neuronal  
731 ensembles. *Nat Neurosci* **2**, 1120-1124 (1999). <https://doi.org/10.1038/16046>
- 732 14 Laricchiuta, D. *et al.* Optogenetic Stimulation of Prelimbic Pyramidal Neurons  
733 Maintains Fear Memories and Modulates Amygdala Pyramidal Neuron  
734 Transcriptome. *Int J Mol Sci* **22** (2021). <https://doi.org/10.3390/ijms22020810>
- 735 15 Bali, P. & Kenny, P. J. Transcriptional mechanisms of drug addiction □ *Dialogues*  
736 *Clin Neurosci* **21**, 379-387 (2019).  
737 <https://doi.org/10.31887/DCNS.2019.21.4/pkenny>
- 738 16 Fernandez-Albert, J. *et al.* Immediate and deferred epigenomic signatures of in  
739 vivo neuronal activation in mouse hippocampus. *Nat Neurosci* **22**, 1718-1730  
740 (2019). <https://doi.org/10.1038/s41593-019-0476-2>

## Molecular impact of electrical stimulation

- 741 17 Marco, A. *et al.* Mapping the epigenomic and transcriptomic interplay during  
742 memory formation and recall in the hippocampal engram ensemble. *Nat Neurosci*  
743 **23**, 1606-1617 (2020). <https://doi.org/10.1038/s41593-020-00717-0>
- 744 18 Trevino, A. E. *et al.* Chromatin and gene-regulatory dynamics of the developing  
745 human cerebral cortex at single-cell resolution. *Cell* **184**, 5053-5069 e5023  
746 (2021). <https://doi.org/10.1016/j.cell.2021.07.039>
- 747 19 Reijmers, L. G., Perkins, B. L., Matsuo, N. & Mayford, M. Localization of a stable  
748 neural correlate of associative memory. *Science* **317**, 1230-1233 (2007).  
749 <https://doi.org/10.1126/science.1143839>
- 750 20 Halder, R. *et al.* DNA methylation changes in plasticity genes accompany the  
751 formation and maintenance of memory. *Nat Neurosci* **19**, 102-110 (2016).  
752 <https://doi.org/10.1038/nn.4194>
- 753 21 Boulting, G. L. *et al.* Activity-dependent regulome of human GABAergic neurons  
754 reveals new patterns of gene regulation and neurological disease heritability. *Nat*  
755 *Neurosci* **24**, 437-448 (2021). <https://doi.org/10.1038/s41593-020-00786-1>
- 756 22 Berto, S. *et al.* Gene-expression correlates of the oscillatory signatures  
757 supporting human episodic memory encoding. *Nat Neurosci* **24**, 554-564 (2021).  
758 <https://doi.org/10.1038/s41593-021-00803-x>
- 759 23 Konopka, G. Cognitive genomics: Linking genes to behavior in the human brain.  
760 *Netw Neurosci* **1**, 3-13 (2017). [https://doi.org/10.1162/NETN\\_a\\_00003](https://doi.org/10.1162/NETN_a_00003)
- 761 24 Berger, M. S. & Ojemann, G. A. Intraoperative brain mapping techniques in  
762 neuro-oncology. *Stereotact Funct Neurosurg* **58**, 153-161 (1992).  
763 <https://doi.org/10.1159/000098989>
- 764 25 Sanai, N., Mirzadeh, Z. & Berger, M. S. Functional outcome after language  
765 mapping for glioma resection. *N Engl J Med* **358**, 18-27 (2008).  
766 <https://doi.org/10.1056/NEJMoa067819>
- 767 26 Brueggeman, L. *et al.* Drug repositioning in epilepsy reveals novel antiseizure  
768 candidates. *Ann Clin Transl Neurol* **6**, 295-309 (2019).  
769 <https://doi.org/10.1002/acn3.703>
- 770 27 Altmann, A. *et al.* A systems-level analysis highlights microglial activation as a  
771 modifying factor in common epilepsies. *Neuropathol Appl Neurobiol* **48**, e12758  
772 (2022). <https://doi.org/10.1111/nan.12758>
- 773 28 Murphy, A. E. & Skene, N. G. A balanced measure shows superior performance  
774 of pseudobulk methods in single-cell RNA-sequencing analysis. *Nat Commun* **13**,  
775 7851 (2022). <https://doi.org/10.1038/s41467-022-35519-4>
- 776 29 Morabito, S. *et al.* Single-nucleus chromatin accessibility and transcriptomic  
777 characterization of Alzheimer's disease. *Nat Genet* **53**, 1143-1155 (2021).  
778 <https://doi.org/10.1038/s41588-021-00894-z>
- 779 30 Caglayan, E., Liu, Y. & Konopka, G. Neuronal ambient RNA contamination  
780 causes misinterpreted and masked cell types in brain single-nuclei datasets.  
781 *Neuron* (2022). <https://doi.org/10.1016/j.neuron.2022.09.010>



## Molecular impact of electrical stimulation

- 782 31 Huang, Y. *et al.* ELK4 exerts opposite roles in cytokine/chemokine production and  
783 degranulation in activated mast cells. *Front Immunol* **14**, 1171380 (2023).  
784 <https://doi.org/10.3389/fimmu.2023.1171380>
- 785 32 Bahl, E. *et al.* Using deep learning to quantify neuronal activation from single-cell  
786 and spatial transcriptomic data. *Nat Commun* **15**, 779 (2024).  
787 <https://doi.org/10.1038/s41467-023-44503-5>
- 788 33 Berto, S., Wang, G. Z., Germi, J., Lega, B. C. & Konopka, G. Human Genomic  
789 Signatures of Brain Oscillations During Memory Encoding. *Cereb Cortex* **28**,  
790 1733-1748 (2018). <https://doi.org/10.1093/cercor/bhx083>
- 791 34 Badimon, A. *et al.* Negative feedback control of neuronal activity by microglia.  
792 *Nature* **586**, 417-423 (2020). <https://doi.org/10.1038/s41586-020-2777-8>
- 793 35 Laprell, L., Schulze, C., Brehme, M. L. & Oertner, T. G. The role of microglia  
794 membrane potential in chemotaxis. *J Neuroinflammation* **18**, 21 (2021).  
795 <https://doi.org/10.1186/s12974-020-02048-0>
- 796 36 Liu, Y. U. *et al.* Neuronal network activity controls microglial process surveillance  
797 in awake mice via norepinephrine signaling. *Nat Neurosci* **22**, 1771-1781 (2019).  
798 <https://doi.org/10.1038/s41593-019-0511-3>
- 799 37 Stowell, R. D. *et al.* Noradrenergic signaling in the wakeful state inhibits  
800 microglial surveillance and synaptic plasticity in the mouse visual cortex. *Nat*  
801 *Neurosci* **22**, 1782-1792 (2019). <https://doi.org/10.1038/s41593-019-0514-0>
- 802 38 Cheadle, L. *et al.* Sensory Experience Engages Microglia to Shape Neural  
803 Connectivity through a Non-Phagocytic Mechanism. *Neuron* **108**, 451-468 e459  
804 (2020). <https://doi.org/10.1016/j.neuron.2020.08.002>
- 805 39 Estevao, C. *et al.* CCL4 induces inflammatory signalling and barrier disruption in  
806 the neurovascular endothelium. *Brain Behav Immun Health* **18**, 100370 (2021).  
807 <https://doi.org/10.1016/j.bbih.2021.100370>
- 808 40 Shen, Y. *et al.* CCR5 closes the temporal window for memory linking. *Nature* **606**,  
809 146-152 (2022). <https://doi.org/10.1038/s41586-022-04783-1>
- 810 41 Chatterjee, S. *et al.* Endoplasmic reticulum chaperone genes encode effectors of  
811 long-term memory. *Sci Adv* **8**, eabm6063 (2022).  
812 <https://doi.org/10.1126/sciadv.abm6063>
- 813 42 Vanrobaeys, Y. *et al.* Mapping the spatial transcriptomic signature of the  
814 hippocampus during memory consolidation. *Nat Commun* **14**, 6100 (2023).  
815 <https://doi.org/10.1038/s41467-023-41715-7>
- 816 43 Rothe, T. *et al.* The Nuclear Receptor Nr4a1 Acts as a Microglia Rheostat and  
817 Serves as a Therapeutic Target in Autoimmune-Driven Central Nervous System  
818 Inflammation. *J Immunol* **198**, 3878-3885 (2017).  
819 <https://doi.org/10.4049/jimmunol.1600638>
- 820 44 Chiu, I. M. *et al.* A neurodegeneration-specific gene-expression signature of  
821 acutely isolated microglia from an amyotrophic lateral sclerosis mouse model.  
822 *Cell Rep* **4**, 385-401 (2013). <https://doi.org/10.1016/j.celrep.2013.06.018>



## Molecular impact of electrical stimulation

- 823 45 Olah, M. *et al.* Single cell RNA sequencing of human microglia uncovers a subset  
824 associated with Alzheimer's disease. *Nat Commun* **11**, 6129 (2020).  
825 <https://doi.org/10.1038/s41467-020-19737-2>
- 826 46 Sheng, R., Chen, C., Chen, H. & Yu, P. Repetitive transcranial magnetic  
827 stimulation for stroke rehabilitation: insights into the molecular and cellular  
828 mechanisms of neuroinflammation. *Front Immunol* **14**, 1197422 (2023).  
829 <https://doi.org/10.3389/fimmu.2023.1197422>
- 830 47 Heck, C. N. *et al.* Two-year seizure reduction in adults with medically intractable  
831 partial onset epilepsy treated with responsive neurostimulation: final results of the  
832 RNS System Pivotal trial. *Epilepsia* **55**, 432-441 (2014).  
833 <https://doi.org/10.1111/epi.12534>
- 834 48 Hammond, T. R. *et al.* Single-Cell RNA Sequencing of Microglia throughout the  
835 Mouse Lifespan and in the Injured Brain Reveals Complex Cell-State Changes.  
836 *Immunity* **50**, 253-271 e256 (2019). <https://doi.org/10.1016/j.immuni.2018.11.004>
- 837 49 Nott, A. *et al.* Brain cell type-specific enhancer-promoter interactome maps and  
838 disease-risk association. *Science* **366**, 1134-1139 (2019).  
839 <https://doi.org/10.1126/science.aay0793>
- 840 50 Hansson, A. C. & Fuxe, K. Time-course of immediate early gene expression in  
841 hippocampal subregions of adrenalectomized rats after acute corticosterone  
842 challenge. *Brain Res* **1215**, 1-10 (2008).  
843 <https://doi.org/10.1016/j.brainres.2008.03.080>
- 844 51 Cullinan, W. E., Herman, J. P., Battaglia, D. F., Akil, H. & Watson, S. J. Pattern  
845 and time course of immediate early gene expression in rat brain following acute  
846 stress. *Neuroscience* **64**, 477-505 (1995). [https://doi.org/10.1016/0306-4522\(94\)00355-9](https://doi.org/10.1016/0306-4522(94)00355-9)
- 848 52 Dobin, A. *et al.* STAR: ultrafast universal RNA-seq aligner. *Bioinformatics* **29**, 15-  
849 21 (2013). <https://doi.org/10.1093/bioinformatics/bts635>
- 850 53 Liao, Y., Smyth, G. K. & Shi, W. featureCounts: an efficient general purpose  
851 program for assigning sequence reads to genomic features. *Bioinformatics* **30**,  
852 923-930 (2014). <https://doi.org/10.1093/bioinformatics/btt656>
- 853 54 Risso, D., Schwartz, K., Sherlock, G. & Dudoit, S. GC-content normalization for  
854 RNA-Seq data. *BMC Bioinformatics* **12**, 480 (2011). <https://doi.org/10.1186/1471-2105-12-480>
- 856 55 Risso, D., Ngai, J., Speed, T. P. & Dudoit, S. Normalization of RNA-seq data  
857 using factor analysis of control genes or samples. *Nat Biotechnol* **32**, 896-902  
858 (2014). <https://doi.org/10.1038/nbt.2931>
- 859 56 Peixoto, L. *et al.* How data analysis affects power, reproducibility and biological  
860 insight of RNA-seq studies in complex datasets. *Nucleic Acids Res* **43**, 7664-  
861 7674 (2015). <https://doi.org/10.1093/nar/gkv736>

## Molecular impact of electrical stimulation

862 57 Robinson, M. D., McCarthy, D. J. & Smyth, G. K. edgeR: a Bioconductor package  
863 for differential expression analysis of digital gene expression data. *Bioinformatics*  
864 **26**, 139-140 (2010). <https://doi.org/10.1093/bioinformatics/btp616>  
865

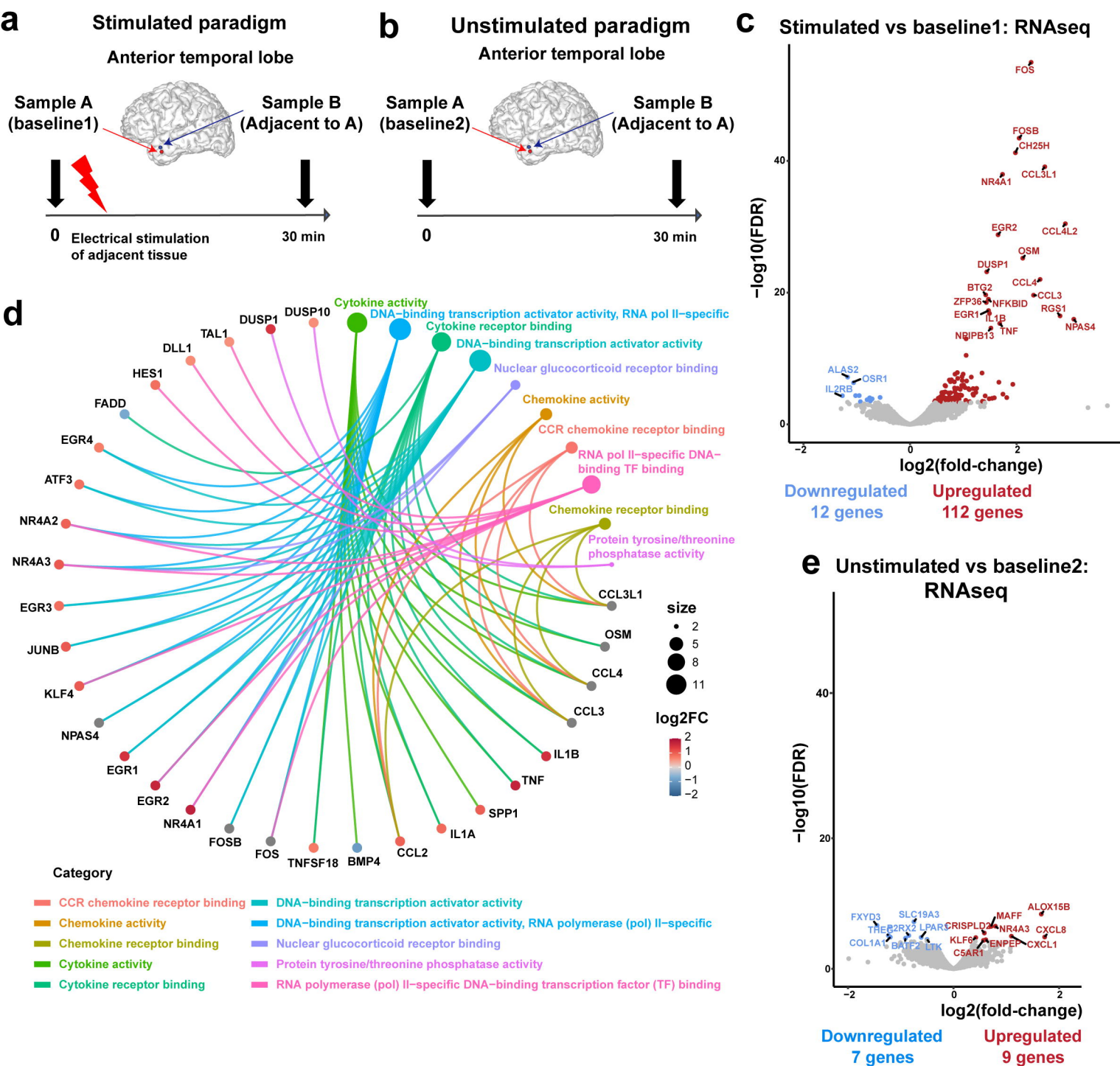
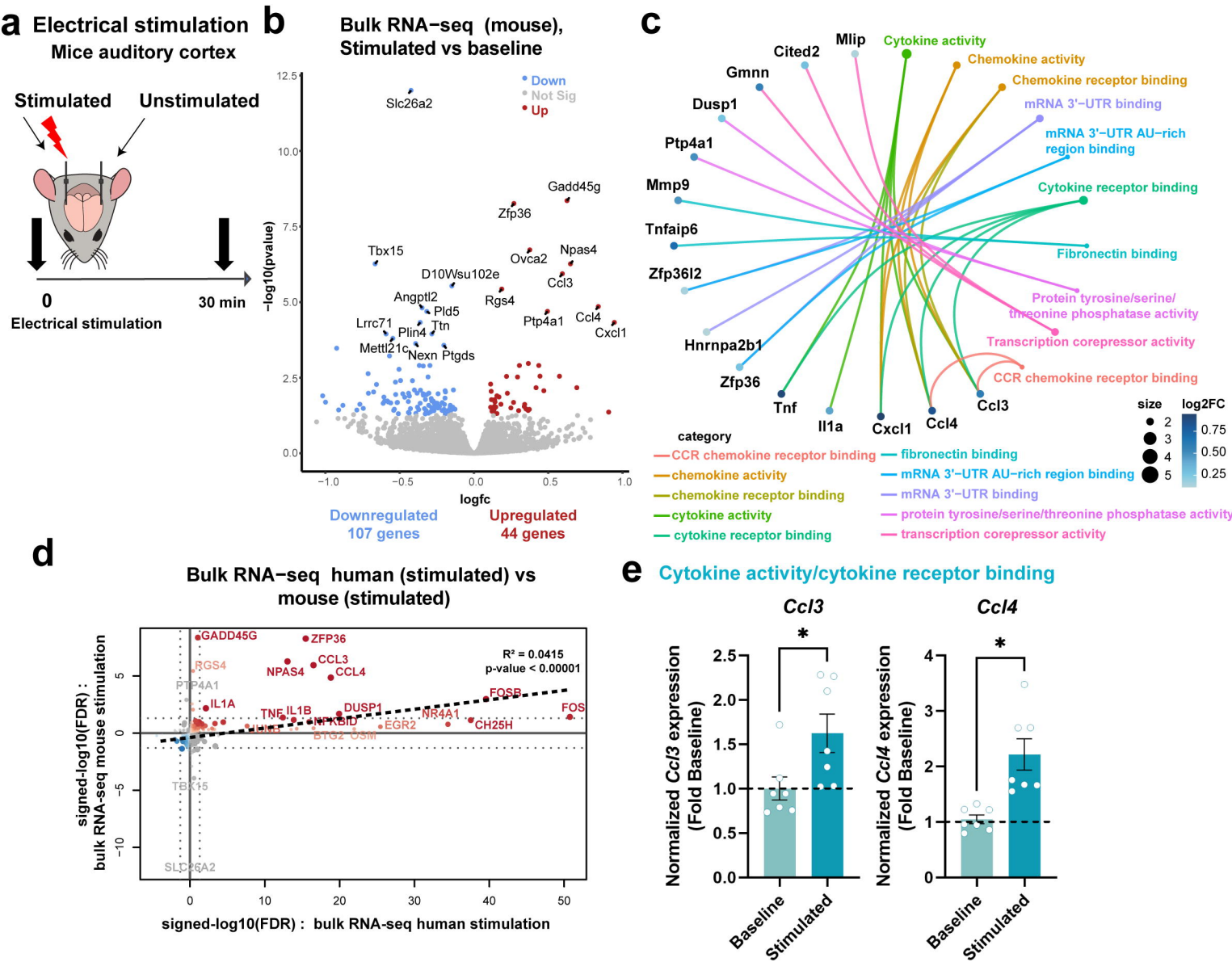


Figure 1



**Figure 2**



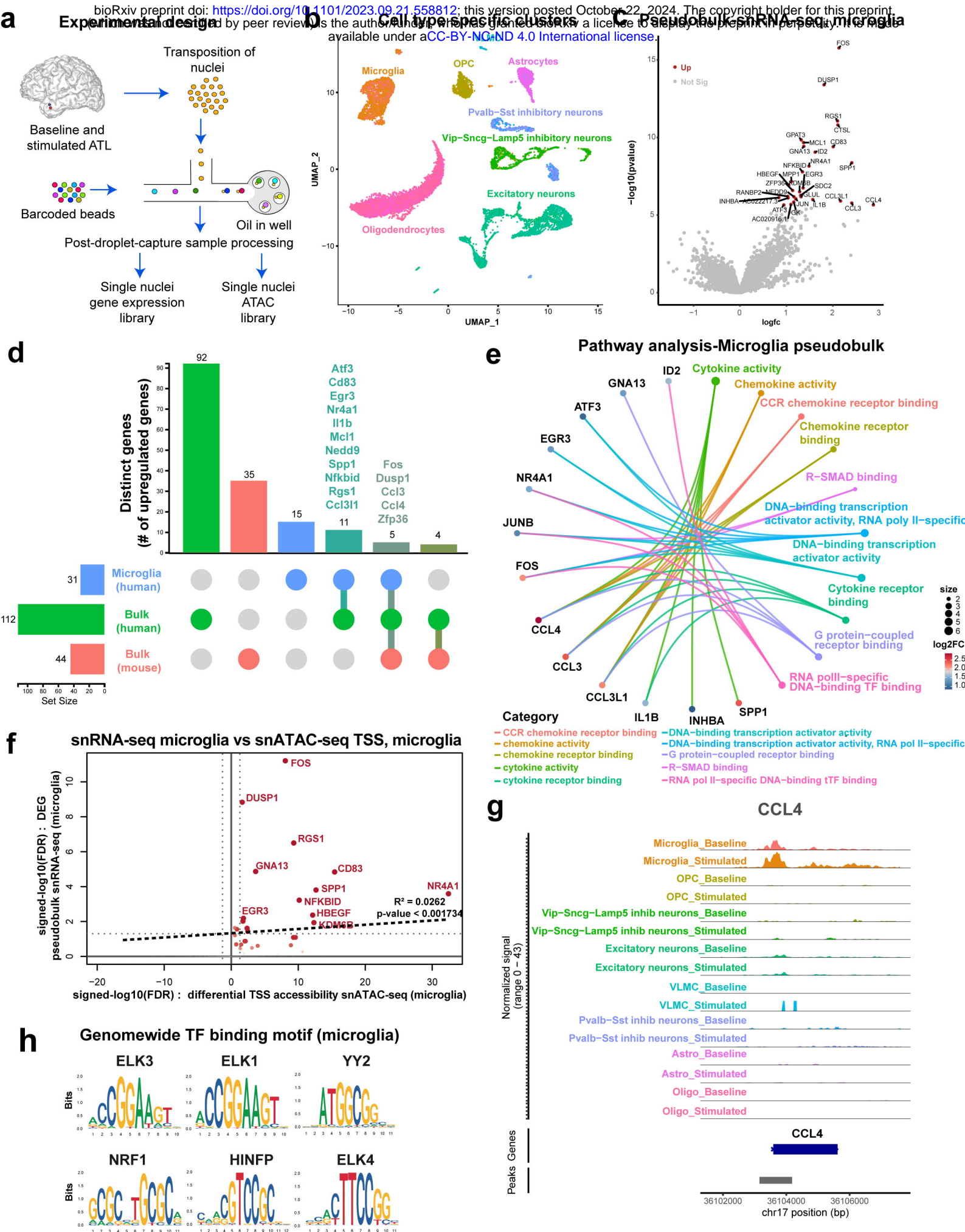
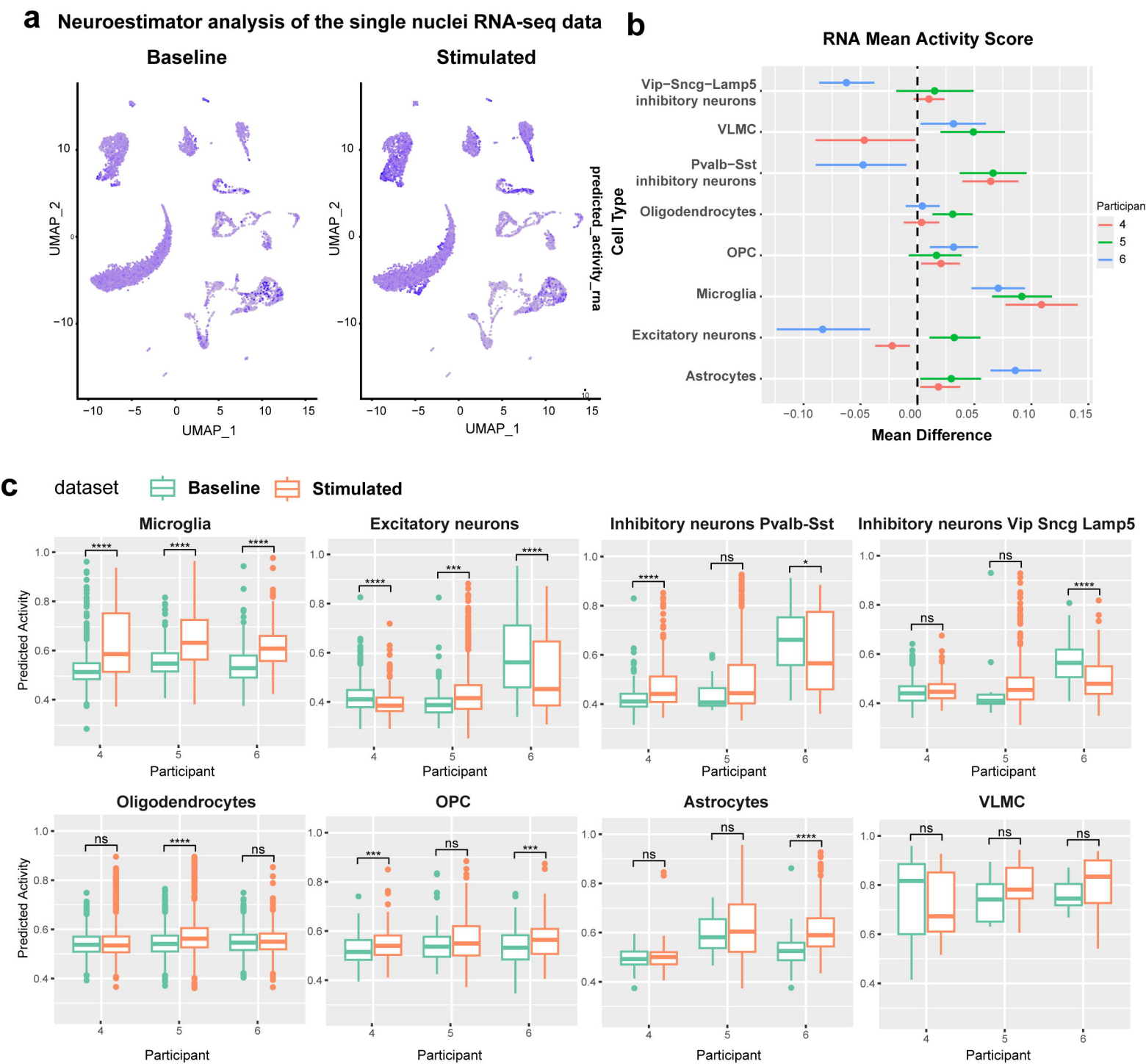


Figure 3



**Figure 4**



